DOI:10.16262/j.cnki.1005-0841.2013.01.002

• Reviews •

Metal oxide/graphene composite anode materials for lithium-ion batteries

LIANG JunFei[a, b] ZHOU Jing [a] GUO Lin [a *]

[a] *School of Chemistry and Environment, Beihang University, Beijing 100191, China*

[b] *Technical Institute of Physics and Chemistry, Chinese Academy of Sciences, Beijing 100190, China*

Abstract Metal oxides, such as SnO_2, Fe_2O_3, Fe_3O_4, CoO, Co_3O_4, NiO, CuO, Cu_2O, MnO, Mn_3O_4, MnO_2, etc., are promising anode materials for lithium-ion batteries (LIBs) due to their high capacity and safety characteristics. However, the commercial utility of metal oxide anodes has been hindered to date by their poor cycling performance. Recent study shows that metal oxide/graphene composites show fascinating cycling performance as anode materials for LIBs. In this review, we summarize the state of research on preparation of metal oxide/graphene composites and their Li storage performance. The prospects and future challenges of metal oxide/graphene composites anode materials for LIBs are also discussed.

Keywords Metal oxides; Graphene; Anode materials; Lithium-ion batteries

1. Introduction

By the 21st century, concerns about the shortage of fossil fuels and the needs to decrease greenhouse gas emissions, coupled with the deterioration of environment, have made people consider the renewable energy in large scale. Meanwhile, the efficient energy storage system is highly required. Since the early 1990s, due to their high capacity, high voltage, light weight, long cycle life, low self-discharge rate and absence of "memory effect", rechargeable lithium-ion batteries (LIBs) have proved themselves as one of the most advanced chemical energy storage devices and hence recently almost dominate the portable electronics market. However, more efforts are still needed to upgrade the performances of LIBs for their further applications in various large electrical appliances such as electric vehicles (EVs) and hybrid electric vehicles (HEVs) as these devices require high capacity, high power density and especially safety. In the case of a battery, electrode materials are determining factor for the battery performance. Currently, graphite is used as an efficient anode material for LIBs because of its long cycle life, abundant material supply and relatively low cost. Even though widely used as an anode material for LIBs, graphite has several disadvantages such as low theoretical capacity (372 mA h g^{-1}), safety problems and so on. The low theoretical capacity of graphite is insuficient to satisfy the increasing demand for batteries with higher capacity [1, 2]. Therefore, scientists have made great efforts to explore alternative anode materials with higher capacity and enhanced safety.

In the past two decades, metal oxides including transition-metal oxides (M_xO_y, M = Fe, Co, Ni, Cu, Mn etc.) and some main group metal oxides (e.g. SnO_2, etc.) have shown their significantly higher capacities, higher potential and better safety characteristics than those of graphite anodes [3—6]. However, the practical application of most metal oxides as anode is hampered by their poor cycle performance, resulting from the serious volume expansion and contraction during the insertion and extraction processes of Li^+ [7, 8]. To address this problem, various methods have been tested [9—13]. Results have shown that hybridizing metal oxides with carbon materials is an effective method to accommodate the strain of volume change during the charge/discharge process [14—19].

Graphene, a one-atom thick and two-di-

* Corresponding author: Tel&. Fax: +86-010-82338162; E-mail: guolin@buaa.edu.cn

mensional closely packed honeycomb lattice, has received numerous investigations from both the experimental and theoretical scientific communities since the experimental observation of single layer by Novoselov and Geim in 2004 [20]. Graphene exhibits a number of intriguing properties, such as excellent intrinsic carrier mobility ($\sim 200000\ cm^2\ V^{-1}\ s^{-1}$) [21], quantum electronic transport [22, 23], high mechanical strength and elasticity [24], superior thermal conductivity [25], chemical stability within a wide range of electrochemical potentials, and so on [26]. Those excellent properties of graphene make it suitable for fabrication into high-performance composites with other anode materials for LIBs. Up to date, by using chemistry solution processes, a lot of papers related to the preparation of metal oxides/graphene composites with improved Li-storage performance have been reported. In this work, we first begin with a brief review of the metal oxides anodes, pointing out the advantages and disadvantages of metal oxides as LIBs anode materials and an efficient method used to improve their electrochemical performance by making composites materials electrode with conductive matrixes, such as graphite, carbon nanotubes, conductive polymers, and so on. Our work focuses on the metal oxides/graphene composites. The synthesis methods and Li storage performances of some familiar metal oxide/graphene composites, such as SnO_2, Fe_2O_3, Fe_3O_4, CoO, Co_3O_4, NiO, CuO, Cu_2O, MnO, Mn_3O_4, MnO_2, etc., will be discussed in separate sections. Finally, the future prospects and challenges of the metal oxide as anode materials for LIBs will be discussed.

2. Metal oxide anode materials

2.1 Classification and Li storage mechanism

Based on the differences of Li storage mechanisms, metal oxides anodes can be divided into three groups, Li-alloy reaction model, displacement reaction model and intercalation/extraction reaction model. The description of each group is mentioned below:

2.1.1 Alloyreaction model

Li-alloy reaction model is based on the reversible charging-discharging in metal oxides. It includes two key processes, i. e. metal alloying and de-alloying. In the first process, the metal oxide is irreversibly converted or reduced to metal that is subsequently dispersed in the matrix of Li_2O. In the next step, the metal reacts with Li^+ to form a variety of Li_xM alloys during the charging process, and the reversible de-alloying process of the Li_xM alloys occurs in the following discharging process. It is just these alloying/de-alloying processes that give the metal oxide Li storage capacity. The overall reaction process for Li-alloy reaction model can be described by the below equations:

$$M_xO_y + 2ye^- + 2yLi^+ \rightarrow x[M]^0 + yLi_2O$$

$$M + xe^- + xLi^+ \leftrightarrow Li_xM$$

Several metal oxides such as Ge-, Sn-, Sb-, and Pb-based oxides follow the alloy model process [27]. For example, a Sn-based oxide first follows the conversion reaction mentioned above to form the Li_2O and metallic Sn, subsequently, the *insitu* formed metallic Sn distributed in Li_2O can store and release Li^+ according to Li-Sn alloying/de-alloying reactions up to the theoretical limit of $Li_{4.4}Sn$ corresponding to a theoretical reversible capacity of 782 mA h g^{-1} based on the mass of SnO_2 [28]. However, its poor cyclic performance caused by large volume changes (up to 300%) during alloying/de-alloying leads to mechanical disintegration and the loss of electrical connection of the active material from current collectors.

2.1.2 Displacement reaction model

In the displacement reaction model, the mechanism involves the reversible formation and decomposition of Li_2O, accompanying the reduction and oxidation of transition metal nanoparticles. The electrochemical reaction mechanism for displacement model can be written as follows:

$$M_xO_y + 2ye^- + 2yLi^+ \leftrightarrow x[M]^0 + yLi_2O$$

M is a transition metal such as Fe, Co, Ni, Mn or Cu, etc. [4]. The final product consists of homogeneous distribution of metal nanoparticles in the range of 1—10 nm embedded in a Li_2O matrix. The electrochemically driven nano-sized confinement of the metal particles is believed to enhance their electrochemical reactivity. However, their application in practical LIBs is significantly hindered by the poor cyclic performance arising from huge volume expansion and severe aggregation of metal oxides during charge/discharge. Another drawback is the large voltage hysteresis between charge and discharge together with poor energy efficiency.

2.1.3 Li^+ intercalation/deintercalation reaction model

For metal oxides with layered structures, Li^+ intercalation/deintercalation can occur in the open channels of layered structures through diffusion, while the structural integrity of the host lattice is normally conserved. The intercalation/deintercalation reactions typically occur around room temperature. The electrochemical reaction mechanism for ntercalation/deintercalation reaction model can be written as follows:

$$M_xO_y + 2ye^- + 2yLi^+ \leftrightarrow Li_yMO_x$$

Several metal oxides such as MoO_2, MoO_3, WO_3 and TiO_2 etc., are examples that follow the intercalation/deintercalation reaction model [27]. For instance, TiO_2 is a common anode metal oxide that follows a typical Li intercalation process with a volume change smaller than 4% in the reaction: $TiO_2 + xLi^+ + xe^- \leftrightarrow 4Li_xTiO_2$ ($0 \leqslant x \leqslant 1$). The lithium intercalation and deintercalation process with a small lattice change ensures its structural stability and cycling life. The lithium intercalation potential is about 1.5 V, thus intrinsically maintaining the safety of the electrode through the avoidance of electrochemical Li deposition. However, its drawback is low specific capacity, poor lithium ionic and electronic conductivity and high polarization, resulting from the slow ionic and electronic diffusion of bulk TiO_2[29].

2.2 Advantages and limitations of metal oxides as anode materials for LIBs

There are several key requirements necessary for an anode material in rechargeable LIBs. The requirements are as follows: (1) the anode material should react with lithium in a reversible manner and the voltage should be low; (2) the anode material should exhibit high capacity; (3) the anode material should exhibit good structural stability which in fact leads to the long cycle life; (4) the anode material should possess good electronic conductivity; (5) the material should be chemically and biologically safe. Based on the above requirements for good anode materials, the advantages and disadvantages of metal oxides as anode materials for LIBs have been mentioned with reference to the currently used graphite anodes. Compared with the graphite anodes, the obvious advantages of the metal oxide anodes are their high capacity and safety characteristics.

Currently, the practical use of metal oxides in LIBs is mainly hampered by their poor long-term cycling stability and intrinsic low charge/ionic conductivity, which indicates that they cannot well meet the requirements mentioned in (3) and (4). For the metal oxides that follow the Li alloy model, such as SnO_2, the practical utilization of them in secondary batteries is hindered due to the dramatic volume change associated with the alloying and de-alloying process. For SnO_2, the reaction of SnO_2 with Li excessively increases the volume which leads to abruption between the yield nanoparticles and the current collector, and hence the disintegration of the electrodes, resulting in poor cycling performance. Similar to the Li-alloying process, metal oxide anodes that follow the conversion reaction of the displacement or intercalation models also yield large volume variation upon the electrochemical cycling. Additionally, the poor electronic conductivity of the metal oxides leads to the polarization of the electrode even at a very low current rate, thus greatly decreases the power density of LIBs.

2.3 Strategy for metal oxide/graphene composite anode

To overcome the problems related with metal oxide anodes for LIBs, several strategies have been developed during the past decades. An efficient strategy is to prepare composite electrodes with other materials, such as graphite [30], carbon nanotubes [31], conductive polymers [32], and so on. These conductive matrixes used to prepare composite electrodes, not only act as physical buffering layer for the large volume changes but also as conductor which could enhance the electronic conductivity of the electrode. Because of its high electrical conductivity and mechanical flexibility, graphene is emerging as one of the most appealing matrices for improving the performance of metal oxides anode. Using this unique 2D ultrathin flexible material, a lot of metal oxide/graphene composite anode materials were reported, in which metal oxides are anchored onto the surface of graphene, or wrapped between graphene layers, or encapsulated by individual graphene nanosheets (GNS). Graphene with 3D structures exhibit a large elastic buffer space to accommodate the volume expansion/contraction of metal oxide particles and confine them during the Li insertion/extraction process. This efficiently prevents the aggregation and cracking or crumbling of the electrode material upon cycling. On the other hand, graphene as an

excellent conductive carbon material in metal oxide electrodes is expected to construct a 3D conductive network among metal oxide particles, and thus maintains the large capacity, good cycling performance and high rate capability [29].

In the following sections, overview on the synthesis and Li storage properties of various metal oxide/graphene composite anode materials will be presented.

3. Synthesis and Li storage properties of metal oxide/graphene composite anode

3.1 SnO_2/graphene composites anode

Since it has been discovered as an important potential anode material for LIBs with high capacity, SnO_2 has attracted wide attention [33]. However, as mentioned above, the biggest problem that hinders the practical use of SnO_2 is the fast capacity fading upon cycling. SnO_2/graphene composites have attracted particular attention because of their improvable electrochemical performances, especially cycling performance.

The SnO_2/graphene composites were first reported by Paek et al. [34]. They prepared a SnO_2/ nanoporous graphene composites anode material with a delaminated structure by assembling SnO_2 nanoparticles on GNS in an ethylene glycol solution. The composites display higher capacity and better cycling performance than that of SnO_2 without graphene (Figure 1). The as-prepared SnO_2/GNS exhibits an initial reversible capacity of 810 mA h g^{-1} and remains at 570 mA h g^{-1} after 30 cycles, while the specific capacity of the bare SnO_2 nanoparticles on the first charge is 550 mA h g^{-1}, but drops rapidly to 60 mA h g^{-1} only after 15 cycles. Another early example is that Yao et al. reported an *in situ* chemical synthesis approach to prepare SnO_2/graphene nanocomposite [35]. The prepared SnO_2/graphene nanocomposites exhibit an initial reversible capacity of 765 mA h g^{-1} and remains at 520 mA h g^{-1} after 100 cycles. Li et al. developed a facile and efficient method to prepare the SnO_2/GNS on the basis of the reduction of graphene oxide (GO) by Sn^{2+}. The prepared SnO_2/GNS exhibits an initial reversible capacity of 541.3 mA h g^{-1} and remains at 377.3 mA h g^{-1} after 35 cycles [36]. Almost at the same time, another SnO_2/GNS were also prepared by oxidation-reduction reaction between GO and Sn^{2+}, and those prepared SnO_2/GNS show improved Li storage performance [37, 38]. Different from the reported methods to prepare the SnO_2/GNS composites based on oxidation-reduction reaction between GO and Sn^{2+}, Liang et al. developed a facile one-step solution route to *in situ* chemically synthetize SnO_2/GNS from GO, DMSO/H_2O and Sn^{4+} (Figure 2) [39]. The mixture of DMSO and H_2O was used as both solvent and reactant. In the reaction system, DMSO not only reduces GO to RGOs, but also results in the formation of SnO_2 nanoparticles facilitated by the presence of H_2O. The as-prepared SnO_2/GNS composites show excellent Li storage performance. More recently, by using the in situ monohydrate vapor reduction to prepare SnO_2 nanocrystals/nitrogen-doped reduced graphene oxide composites material (Figure 3), Zhou et al. have enabled SnO_2 nanocrystals to approach the theoretical capacity of SnO_2 as an anode material for LIBs [40]. The as-obtained hybrid materials exhibit excellent properties in terms of cycling performance and rate capability as well as cycle life for LIBs, benefiting from the nano-sized SnO_2 particles, the highly conductive graphene, and the Sn-N bond formed between graphene and SnO_2 nanocrystals. Prabakar developed a facile *in situ* solution-based self-assembly procedure to synthesize well-ordered and densely packed alternating graphene layers with crystalline SnO_2 nanoparticles [41].

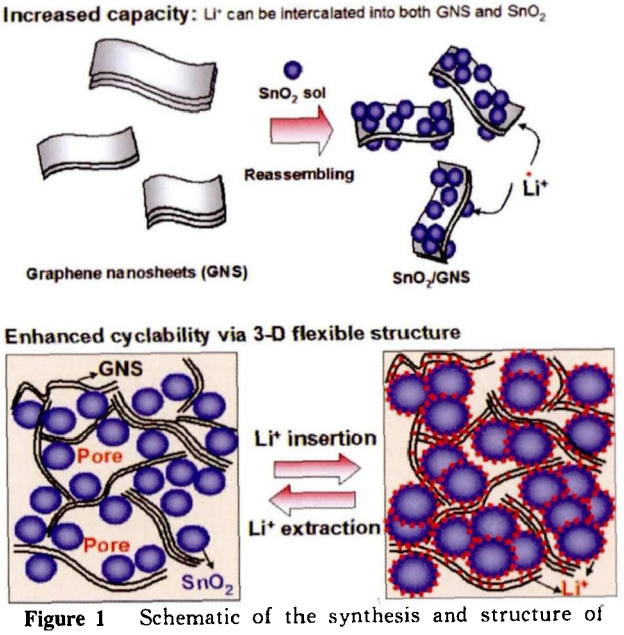

Figure 1 Schematic of the synthesis and structure of GNS/SnO_2. Reproduced from [34]. Copyright 2010, American Chemical Society.

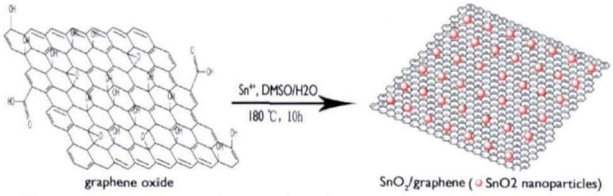

Figure 2 Scheme illustration for the synthesis of SnO_2/GNS nanocomposites. Reproduced from [39]. Copyright 2012, American Chemical Society.

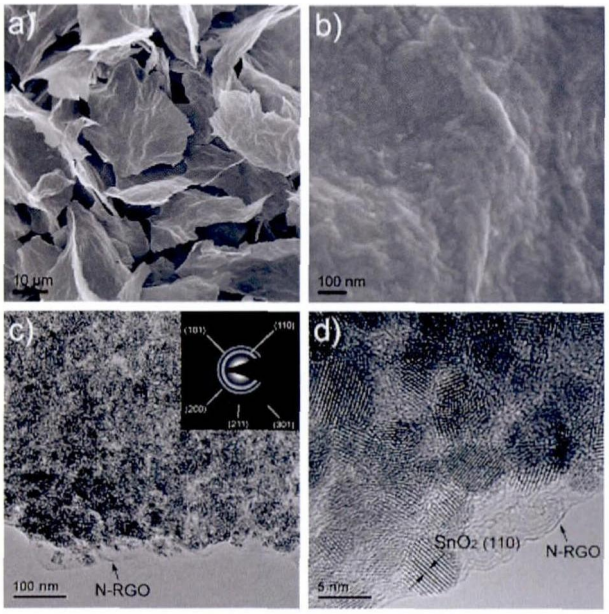

Figure 3 (a, b) SEM (a) and high-magnifi cation SEM (b) images of SnO_2 NCN-RGO. (c) TEM image of SnO_2 NCN-RGO. Inset: The corresponding SAED pattern. (d) HRTEM image of SnO_2 NCN-RGO. Reproduced from [40]. Copyright 2013, John Wiley & Sons, Inc.

The opposite polarity of the SnO_2-anchored graphene and amine-functionalized graphene facilitates electrostatic pre-aligning, which eliminates macropores and a significant fraction of micro-mesopores after thermal reduction. The SnO_2-anchored graphene/amine-functionalized graphene displays excellent Li-storage capability with surprisingly stable capacity retention (872 mA h g^{-1} after 200 cycles at a rate of 100 mA g^{-1}). Wang et al. reported a system-level strategy of fabrication of reduced graphene oxide (RGO)/SnO_2 composite-based anode for LIBs [42]. They designed a new RGO/SnO_2-based electrode composite through coating it by a functional buffer layer and cross-linking the buffer layer and binder to address the issue of poor cyclic performance of SnO_2-based anodes (Figure 4). The prepared RGO/SnO_2 composite exhibited a good cyclic performance with capacity up to 718 mA h g^{-1} at current density of 100 mA g^{-1} after 200 cycles and an excellent rate performance.

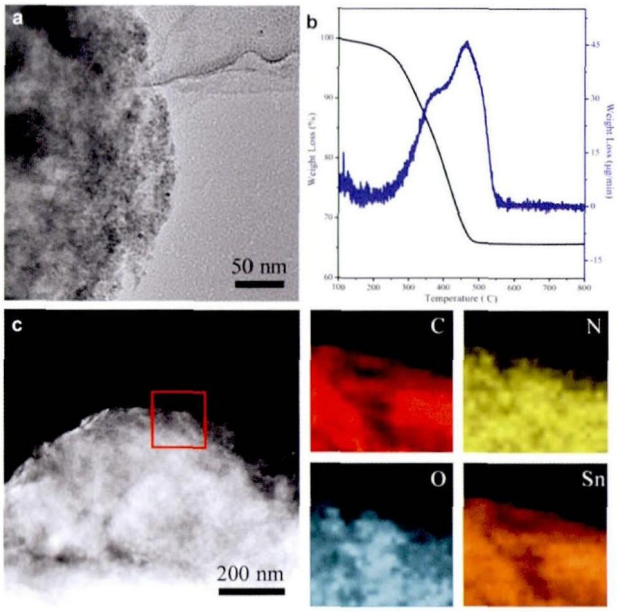

Figure 4 Characterization of PD-coated RGO/SnO_2 composite. TEM image (a), TG and DTG curves (b), DF-STEM image and corresponding element mapping images of C, N, O, and Sn (c). Reproduced from [42]. Copyright 2013, American Chemical Society.

Compared with SnO_2 nanoparticles/graphene composites, the SnO_2 with specific morphologies hybrid with GNS shows better Li storage performance, and some papers about this area were reported [43—46]. Ding et al. developed a hydrothermal method to directly grow SnO_2 nanosheets on graphene oxide support that is subsequently reduced to graphene [43]. The unique SnO_2/graphene hybrid structure exhibits enhanced Li storage properties compared to the pure SnO_2 nanosheets. The prepared SnO_2 nanosheets/graphene composites show reversible capacity of 518 mA h g^{-1} after 50 cycles at 400 mA g^{-1}. Another example of specific morphologies SnO_2/graphene composites is that Kim et al. controlled surface charge to prepare echinoid-like SnO_2 uniformly decorated on GNS [44]. The echinoid-like SnO_2/GNS composite retains a reversible capacity of 634 mA h g^{-1} after 50 cycles. Xu et al. developed a facile one-step hydrothermal procedure to prepare hybrid materials of SnO_2 nanorods on graphene sheets [45]. Compared with bare SnO_2 nanorods, the SnO_2 nanorods/GNS shows higher reversible specific capacity and more outstanding cycling stability. The prepared SnO_2 nanorods/GNS exhibits an initial dis-

charge capacities of 1147 and 928 mA h g^{-1} at current densities of 100 and 200 mA g^{-1}, respectively. After 50 cycles, the capacities are 710 and 574.6 mA h g^{-1} with a capacity loss of 0.3% per cycle with the current density of 100 and 200 mA g^{-1} while the initial specific capacity of the bare SnO_2 nanorods is 1610 and 1027 mA h g^{-1}, dropping rapidly to 237 and 105 mA h g^{-1} after 50 cycles at the same current densities. Recently, Zhou et al. synthesized graphene enwrapped SnO_2 hollow nanospheres as robust high-capacity anode materials for LIBs [46]. The as-obtained SnO_2 hollow nanospheres/graphene exhibits stable cycle ability and superior high-rate capability. A specific capacity as high as 696 mA h g^{-1} is obtained even after 300 cycles under 0.5 A g^{-1}.

Owing to their attractive characteristics, LIBs are not only widely used in conventional electronic devices [47, 48], but also hold great promise for powering flexible electronics if they can be fabricated into a flexible form [49]. Some reported metal oxide/graphene composites films show great potential for flexible LIBs. By coupling a simple filtration method and a thermal reduction together, Liang et al. prepared a flexible free-standing SnO_2/graphene nanocomposites film (Figure 5) [50]. Compared with the pure SnO_2 nanoparticles, the nanocomposites exhibited a better cycling stability, because the graphene with high mechanical strength and elasticity can work as a buffer to prevent the volume expansion and contraction of SnO_2 nanoparticles during the Li^+ insertion/extraction process. Meanwhile, compared with single graphene films, the GSP showed a higher capacity because of the hybridizing with higher capacity SnO_2 nanoparticles. By using 7, 7, 8, 8-tetracyanoquinodimethane anion as both the nitrogen source and the complexing agent, Wang et al. developed a new facile route to fabricate N-doped graphene-SnO_2 sandwich papers [51]. When used in LIBs, the prepared paper exhibits a very large capacity, high rate capability, and excellent cycling stability. The N-doped graphene-SnO_2 sandwich papers keep a high capacity of 910 mA h g^{-1} after 50 cycles at current densities of 50 mA g^{-1}. They indicate that the enhanced electrochemical performances of the sandwich papers can be attributed to the structural features that provide a large number of surface defects induced onto the graphene by N-doping, excellent electronic conductivity, short transportation length for both lithium ions and electrons, and enough elastomeric space to accommodate volume changes upon Li^+ insertion/extraction.

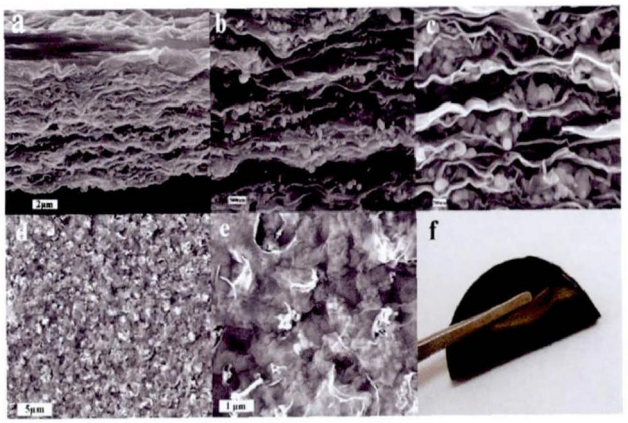

Figure 5 (a-c) Low-, middle-, and high-resolution FESEM cross section images of the paper; (d, e) low and high magnification FESEM top view images of the paper; (f) photograph of the as-prepared GOSP. Reproduced from [50]. Copyright 2012, American Chemical Society.

As a group of novel porous materials with advantages of low mass density, continuous porosity, high surface area and high electrical conductivity, metal oxide/graphene xerogels can be explored as novel anode materials for LIBs [52]. Liang et al. successfully prepared a novel 3D macroscopic SnO_2/graphene aerogel, with interconnected macroporous networks, in high yield and on a large scale by a facile one-step method (Figure 6) [53]. The reduction of GO to graphene, the self-assembly of graphene sheets to form 3D macroscopic aerogel and the *in situ* uniform deposition of SnO_2 nanoparticles were realized in one step. Moreover, the electrochemical results show the facilely separable and low-cost SnO_2/graphene aerogel provides excellent capacity and cyclic stability. Huang et al. developed a method to prepare 3D hierarchical SnO_2/graphene frameworks by the *in situ* synthesis of 2D SnO_2/graphene nanosheets followed by hydrothermal assembly [54]. These SnO_2/graphene frameworks exhibited a 3D hierarchical porous architecture with mesopores ($\approx$3 nm), macropores (3—6 μm), and a large surface area (244 m^2 g^{-1}), which not only effectively prevented the agglomeration of SnO_2 nanoparticles, but also facilitated fast ion and electron transport in 3D path-

ways. As a consequence, SnO_2/graphene frameworks exhibited a high capacity of 830 mA h g^{-1} for up to 70 charge-discharge cycles at 100 mA g^{-1}.

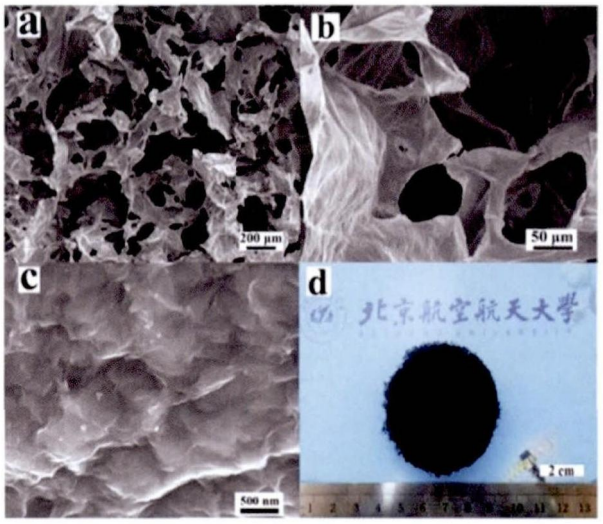

Figure 6 (a—c) Low-, middle- and high-resolution FESEM cross-section images of the SGA; (d) photograph of the scaled-up synthesis of the SGA [53]. Copyright 2013, The Royal Society of Chemistry.

3.2 Fe, Co and Ni oxides/graphene composites anode

It is reported that 3D transition-metal oxides such as nickel oxides, cobalt oxides, and iron oxides exhibit reversible capacities about three times larger than those of graphite [2, 55]. Similar to the SnO_2 anode, the notorious problems of 3D transition-metal oxides as anode materials are the poor cycling performance. Recently, the enhanced electrochemical performance of iron, cobalt and nickel oxides has been reported through the fabrication of composites with graphene.

Zhang et al. developed a green and effective methodology to prepare Fe_2O_3/graphene composites [56]. The essence of their method was that ferrous ions could serve as both reductant and the iron source for Fe_2O_3. As anode materials for LIBs, the prepared Fe_2O_3/graphene composites achieved high reversible capacities of about 800 mA h g^{-1} after 100 cycles at a charge-discharge rate of 0.2 C. Moreover, they delivered rate capacities as high as 420 mA h g^{-1} at a rate of 5 C. They indicated the improved performance toward the storage of Li^+ was ascribed to graphene sheets, which acted as volume buffers and electron conductors. Using a two-step synthesis by homogeneous precipitation and subsequent reduction of the GO with hydrazine under microwave irradiation to yield RGO platelets decorated with Fe_2O_3 nanoparticles, Zhu et al. prepared a RGO/Fe_2O_3 composite (Figure 7) [57]. As an anode material for LIBs, the RGO/Fe_2O_3 composite exhibited discharge and charge capacities of 1693 and 1227 mA h g^{-1}, respectively, with good cycling performance and rate capability. Characterization shows that the Fe_2O_3 nanoparticles are uniformly distributed on the surface of the RGO platelets in the composite. The total specific capacity of RGO/Fe_2O_3 is higher than the sum of pure RGO and nanoparticle Fe_2O_3, indicating a positive synergistic effect of RGO and Fe_2O_3 on the improvement of electrochemical performance. Du et al. synthesized a-Fe_2O_3/RGO composite by a hydrothermal method. $Fe(OH)_3$ sol is creatively employed as the precursor and no nucleating agent is employed to help Fe^{3+} change to $Fe(OH)_3$ [58]. In the hydrothermal process, $Fe(OH)_3$ sol transforms to a-Fe_2O_3 particles and GO becomes RGO with hydrazine hydrate. The as-prepared a-Fe_2O_3/RGO containing 73% a-Fe_2O_3 exhibits the highest reversible specific capacity of 950 mA h g^{-1} after 70 cycles at a current density of 100 mA g^{-1}. When the current density is 800 mA g^{-1}, the capacity still remains as 700 mA h g^{-1}, showing superior rate capability. More recently, Chen et al. synthesized a Fe_2O_3/graphene composite by a one-pot surfactant governed approach under mild wet-chemical conditions [59]. The Fe_2O_3 nanoparticles with relatively uniform size were encapsulated by graphene layers and were able to form core-shell nanostructures (Figure 8).

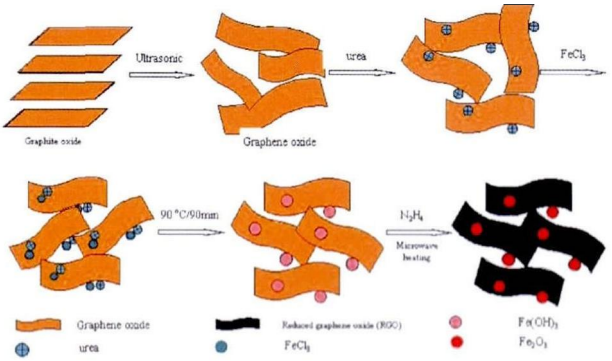

Figure 7 Scheme of RGO/Fe_2O_3 composite forming mechanism [57]. Copyright 2011, American Chemical Society.

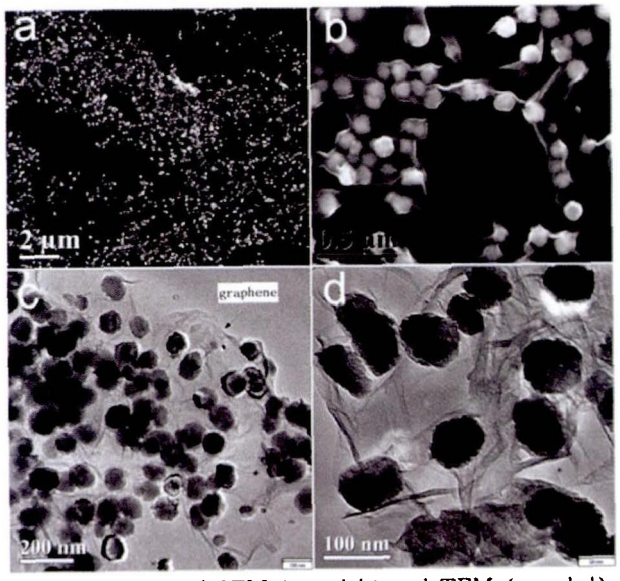

Figure 8 Typical SEM (a and b) and TEM (c and d) images of HNGNS composites [59]. Copyright 2013, The Royal Society of Chemistry.

The as-prepared Fe_2O_3/graphene core-shell nanostructures exhibited a high reversible specific capacity of 1040 mA h g^{-1} at a current density of 200 mA g^{-1} (0.2 C) after 180 cycles and excellent rate capability and long cycle life. Furthermore, a reversible capacity as high as 500 mA h g^{-1} was still achieved after 200 cycles even at a high rate of 6 C.

Yang et al. prepared Co_3O_4/graphene with core-shell structure by electrostatic forces [60]. The method enables a good encapsulation of electrochemically active metal oxide nanoparticles by graphene sheets, thus leading to remarkable Li-storage performance, including highly reversible capacity and excellent cycle performance. Wu et al. developed a facile strategy to synthesize a composite of graphene anchored with Co_3O_4 nanoparticles as an anode material for LIBs [61]. The Co_3O_4 nanoparticles obtained are 10—30 nm in size and homogeneously anchored on graphene. They indicate that the flexible structure of 2D graphene sheets and the strong interaction between Co_3O_4 nanoparticles and graphene sheets in Co_3O_4/graphene composite are beneficial for efficiently preventing volume expansion/contraction and aggregation of Co_3O_4 during Li charge/discharge process. Therefore, such a composite is capable of effectively utilizing the good conductivity, high surface area, mechanical flexibility, and good electrochemical performance of graphene as well as the large electrode/electrolyte contact area, short path length for Li^+ transport, and good stability for nanostructured Co_3O_4 particles. As a result, the Co_3O_4/graphene composite exhibits a large reversible capacity (~ 935 mA h g^{-1} after 30 cycles), excellent cyclic performance, high coulombic efficiency (above ~ 98%), and good rate capability. Chen et al. prepared a Co_3O_4-graphene sheet-on-sheet composite by a microwave-assisted method [62]. Graphene nanosheets were tightly stacked with porous Co_3O_4 nanosheets, whereby reassembly of GNS to graphite platelets was prevented. The sheet-on-sheet composite showed a very large capacity of 1235 mA h g^{-1} and distinguished superior rate capabilities. A high capacity of 931 mA h g^{-1} was still observed at a large rate of 5 C (4450 mA g^{-1}). They indicate the complementary synergetic effect of the composite may be attributed to the prevented aggregation of graphene nanosheets, which were separated and stabilized by Co_3O_4 nanosheets and increased electrical conductivity and mechanical stability of Co_3O_4 porous nanosheets in the presence of graphene nanosheets. Li et al. developed a simple and scalable preparation approach of Co_3O_4/graphene nanocomposites via a chemical reduction process of GO in a $NaBH_4$ solution [63]. The cycle performance was determined for up to 60 cycles with an excellent cycle stability and high rate capability. The Co_3O_4/graphene composites demonstrated enhanced Li^+ intercalation properties for not only superior electronic conductivity but also layer-structure of graphene and possessed a specific discharge capacity of 941 mA h g^{-1} in the initial cycle and 740 mA h g^{-1} after 60 cycles.

Zou et al. reported a hydrothermal preparation of NiO/graphene sheet-on-sheet and nanoparticle-on-sheet nanostructures [64]. The sheet-on-sheet nanocomposite showed highly reversible large capacities at a common current of 0.1 C and good rate capabilities. A large initial charge capacity of 1056 mA h g^{-1} was observed for the sheet-on-sheet composite at 0.1 C, which decreased by only 2.4% to 1031 mA h g^{-1} after 40 cycles of discharge and charge. They indicate the cycling performance of the NiO/graphene sheet-on-sheet nanostructures is better than that of NiO nanosheets, graphene nanosheets, NiO-graphene nanopar-

ticle-on-sheet, and previous carbon/carbon nanotube supported NiO composites. They believe that the mechanical stability and electrical conductivity of NiO nanosheets are increased by graphene nanosheets, the aggregation or restacking of which to graphite platelets are, on the other hand, effectively prevented by NiO nanosheets. Kottegoda et al. prepared a graphene/NiO nanocomposite by a controlled hydrothermal method and the as-prepared nanocomposites showed high rate capability and long cycle life as anode in LIBs [65]. A capacity of 450 mA h g^{-1} after 100 cycles at 1 C and a discharge capacity of 185 mA h g^{-1} at 20 C were obtained. They indicate the graphene plays a dual role in delivering good performance. Firstly, graphene works as a supporting material for the nanostructured NiO particles to give good mechanical stability for lithium insertion and de-insertion. Secondly, as a Li^+ insertion material, the graphene provides good energy storage capacity.

3.3 CuO/graphene composites anode

Although the electrochemical performance of CuO/graphene composites as LIBs anode materials have not been widely investigated, their advantages compared with the bare CuO anodes have been already confirmed by some literature [66—68]. Wang et al. synthesized a self-assembled CuO/graphene urchin-like structure by a simple solution method (Figure 9) [66]. Compared with pure CuO urchin-like structure, the as-prepared CuO/graphene nanocomposite exhibits a remarkably enhanced cycling performance and rate performance. During all the 100 discharge-charge cycles under a current density of 65 mA g^{-1}, the CuO/graphene electrode can stably deliver a reversible capacity of 600 mA h g^{-1}. At a high current density of 6400 mA g^{-1}, the specific charge capacity of the CuO/graphene nanocomposite is still as high as 150 mA h g^{-1}, which is three times larger than that of graphene (48 mA h g^{-1}), while that of CuO is nearly null under the same current density. Mai et al. prepared CuO/graphene composite by an *in situ* chemical synthesis approach [67]. The CuO/graphene composite exhibits a reversible capacity of 561.4 mA h g^{-1}. After 50 cycles the discharge capacity still remains at 423 mA h g^{-1}, which is about 75.3 % retention of the reversible capacity, while the specific capacity of the bare CuO on the first charge is 752.4 mA h g^{-1}, dropping rapidly to 226 mA h g^{-1} only after 50 cycles. Lu et al. prepared CuO/graphene layer-by-layer hybrid nanostructures by a fast microwave irradiation method [68]. These CuO nanostructures were uniformly dispersed on GNS, forming layer-by- layer nanostructures after drying and stacking. When used as anode materials for LIBs, the CuO/GNS composites showed substantially enhanced lithium-storage capacities compared to CuO materials and GNS.

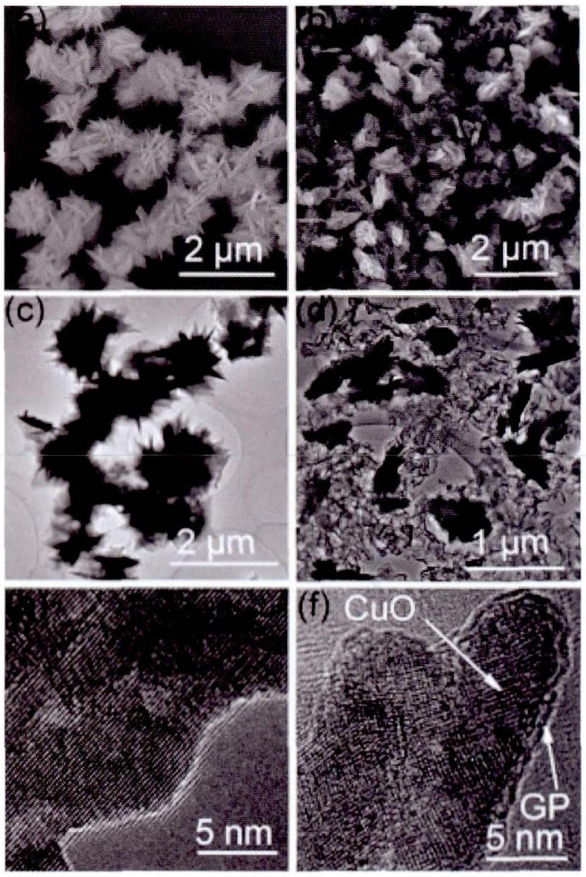

Figure 9 SEM and TEM images of the as-prepared CuO (a, c, e) and CuO/graphene (b, d, f) [66]. Copyright 2010, The Royal Society of Chemistry.

3.4 Mn oxide/graphene composites anode

In the past decade, Mn oxide has been investigated as an effective anode material for LIBs because of its low cost, low toxicity and high capacity. The electrochemical performance of the Mn oxide has been significantly improved by the fabrication of composites with graphene [69—73]. Wang

et al. developed two-step solution-phase reactions to form composites of Mn_3O_4 nanoparticles on RGO sheets for LIBs applications (Figure 10) [69]. Selective growth of Mn_3O_4 nanoparticles on RGO sheets, compared with free Mn_3O_4 particle growth in solution, allowed for the electrically insulating Mn_3O_4 nanoparticles to be wired up to a current collector through the underlying conducting graphene network. The Mn_3O_4 nanoparticles formed on RGO show a high specific capacity up to ~ 900 mA h g^{-1}, near their theoretical capacity, with good rate capability and cycling stability, owing to the intimate interactions between the graphene substrates and the Mn_3O_4 nanoparticles. Yu et al. prepared a free-standing layer-by-layer assembled hybrid graphene/MnO_2 nanotube thin films by an ultrafiltration technique [70]. The graphene/MnO_2 nanotube films as anode present excellent cycle and rate capabilities with a reversible specific capacity based on electrode composite mass of 495 mA h g^{-1} at 100 mA g^{-1} after 40 cycles with various current rates from 100 to 1600 mA g^{-1}. On the contrary, graphene-free MnO_2 nanotube electrodes demonstrate only 140 mA h g^{-1} at 80 mA g^{-1} after 10 cycles. Furthermore, at a high current rate of 1600 mA g^{-1}, the charge capacity of graphene/MnO_2 nanotube film reached 208 mA h g^{-1}. Guo et al. fabricated a hierarchically nanostructured composite material of layered birnessite-type MnO_2/polymerized poly (3, 4-ethylenedioxythiophene)/graphene that can significantly improve LIBs performance due to its unique structure and composition, each component of which plays a unique role [71]. The composites shows a discharge capacity of 1105 mA h g^{-1} on the second cycle, remaining at as high as 948 mA h g^{-1} after 15 cycles. Even increasing the charge/discharge rate, the composites can still deliver a reversible capacity of 930, 836, and 698 mA h g^{-1} at rates of 100, 200, and 400 mA g^{-1}, respectively. Hsieh et al. fabricated a MnO/graphene composite through a simple chemical-wet impregnation followed by the thermal reduction route. The MnO-attached GNS anode delivers a reversible capacity of 635 mA h g^{-1} at 0.2 C [72]. Li et al. synthesized a nanocomposite of Mn_3O_4 wrapped in graphene sheets via a facile, effective, energy-saving, and scalable microwave hydrothermal technique [73]. The as-prepared nanocomposites shows a high specific capacity of more than 900 mA h g^{-1} at 40 mA g^{-1}, and excellent cycling stability with no capacity decay can be observed up to 50 cycles.

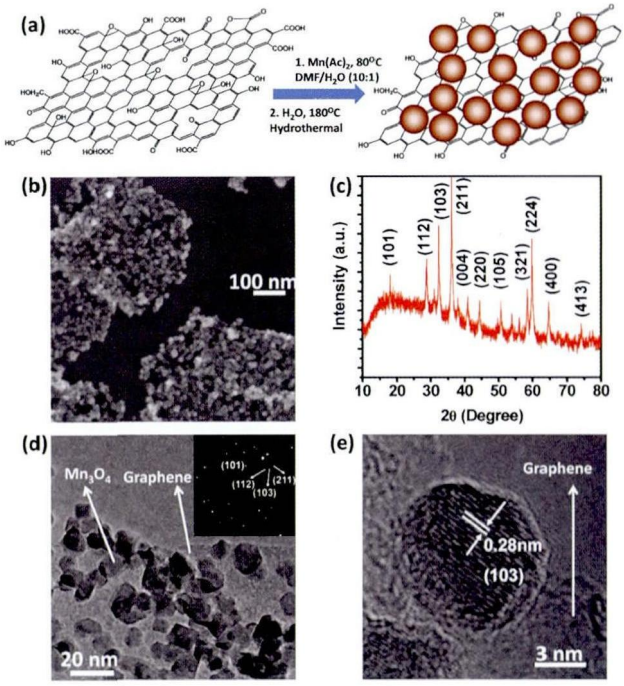

Figure 10 Mn_3O_4 nanoparticles grown on GO. (a) Schematic two-step synthesis of Mn_3O_4/RGO. (b) SEM image of Mn_3O_4/RGO hybrid. (c) XRD spectrum of a packed thick film of Mn_3O_4/RGO. (d) TEM image of Mn_3O_4/RGO; inset shows the electron diffraction pattern of the Mn_3O_4 nanoparticles on RGO. (e) High-resolution TEM image of an individual Mn_3O_4 nanoparticle on RGO [69]. Copyright 2010, American Chemical Society.

4. Conclusion and future prospects

We have reviewed the recent advance in synthesis and applications of metal oxide/graphene composite materials for LIBs. The critical role of graphene in the composites is due to its unique structures and properties such as high surface area, ultra-thin thickness, excellent electrical conductivity, superior thermal conductivity, high mechanical strength and elasticity, chemical stability within a wide range of electrochemical potentials and so on. Therefore, graphene can serve as an ideal 2D support for depositing or assembling very

small nanoparticles with well-defined structures, creating various graphene-based materials with excellent application performance. The improved performance of metal oxide/graphene composites as anode for LIBs should be attributed to the unique features of the composites. On the one hand, the main reason for the rapid fading of metal oxide electrode is that the large volume change of the metal oxide occurs during the charge-discharge cycle, leading to cracking and pulverization of the electrode. Graphene have excellent mechanical properties. A super flexiblecoating made of high mechanically graphene sheets covered with the metal oxide nanocrystals not only provides an elastic buffer space to accommodate the volume changes upon Li^+ insertion/extraction but also efficiently prevents the aggregation of the nanoparticles and the cracking or crumbling of the electrode material; therefore, a better cycle stability can be obtained. Even though volume expansion still exists, the electrode will not pulverize as the graphene sheets can deform resiliently to accommodate such volume changes. On the other hand, the graphene sheets with high surface area can build a better conductive network which could promote the electron transfer during the lithiation and delithiation process. In the composites, the electronic transport speed is effectively accelerated compared with the single metal oxide nanocrystals. Futhermore, the graphene sheets can provide a continuous conductive path in between the metal oxide nanocrystals, which can reduce the particle-particle interface resistance effectively. The *in situ* forming of the metal oxide nanocrystals, the electrostatic attraction between electron-rich Sn atoms and electron-unsaturated carbon atoms of graphene enable the metal oxide nanocrystals to be firmly anchored on graphene surface and thus enhance the conjunction stability of the composites. The close contact between the metal oxide nanoparticles and the super electroconductive graphene can also minimize the electrical isolation of nanoparticles during battery cycles. The above synergetic effects arising from the particular structure of metal oxide/graphene composites is responsible for the excellent electrochemical performance of the composites anode. Due to these synergistic effects, integration of metal oxides and graphene in a composite fully uses each active component and consequently achieves excellent electrochemical performance in LIBs through materials design and fabrication. Despite the short period of research, metal oxide/graphene composites with various structures have show greatly improved electrochemical performance as electrodes of LIBs, such as high capacity, improved rate capability, improved cycling stability. It is worth to note that, among the various applications of metal oxide/graphene composites, LIBs have so far attracted more and more attention and are very likely to be commercially used in the near future through further optimization toward designing the metal oxide/graphene materials. However, several important challenges still urgently need to be overcome: (1) For LIB applications, the fast charge transfer processes in the electrode is very impotent. However, in most reported metal oxide/graphene composites, the charge transfer is slow because of the weak interface interaction between graphene and metal oxides. Therefore, a good understanding of surface chemistry on graphene and metal oxides is important to increase the interfacial interactions and thus achieve fast charge transfer. (2) Rational design and control of the morphology and phase composition of metal oxides on graphene can ensure reproducibility and better understanding of the structure-property relationships. However, it is still a challenge to control of the morphology and phase composition of metal oxides in the preparation process. (3) Understanding and clarifying the effects of graphene on the LIBs performance of metal oxide/graphene composites are also important. However, the report about this field is rare. (4) Graphene with unique properties of high mechanical strength and elasticity, lightweight and flexible will open up enormous opportunities for the fabrication of thin and flexible electrodes for LIBs. (5) New approaches to fabricate metal oxide/graphene composites is need to be developed, which must involve a combined focus on controlled synthesis and improved LIB performance of novel

composite materials. (6) Considering the final industrial implementation, the successful application of metal oxide/graphene composites requires a comprehensive improvement in methodology and performance and better compatibility of the composites for use in the whole LIB device, not merely high performance of the composite electrodes in some aspects. (7) The large-scale, low-cost and simple production of metal oxide/graphene is still a challenge. With continuous exploitation, it is believed that metal oxide/graphene composite materials for LIBs will realize many practical applications.

Acknowledgment

This work was financially supported by the National Science Foundation for Distinguished Young Scholar (50725208), National Natural Science Foundation of China (11079002 & 51272012) and Specialized Research Fund for the Doctoral Program of Higher Education (20111102130006).

References

[1] Winter M, Besenhard J O, Spahr M E, et al. Insertion electrode materials for rechargeable lithium batteries. Adv Mater, 1998, 10 (10): 725—763.

[2] Wei W, Wang Z, Liu Z, et al. Metal oxide hollow nanostructures: fabrication and Li storage performance. J Power Sources, 2013, 238: 376—387.

[3] Thackeray M M, David W I F, Bruce P G. Lithium insertion into manganese spinels. Mater Res Bull, 1983, 18 (4): 461—472.

[4] Poizot P, Laruelle S, Grugeon S, et al. Nano-sized transition-metal oxides as negative-electrode materials for lithium-ion batteries. Nature, 2000, 407: 496—499.

[5] Cabana J, Monconduit L, Larcher D, et al. Beyond intercalation-based Li-ion batteries: the state of the art and challenges of electrode materials reacting through conversion reactions. Adv Mater, 2010, 22 (35): E170—E192.

[6] Wang X, Wu X L, Guo Y G, et al. Synthesis and lithium storage properties of Co_3O_4 nanosheet-assembled multishelled hollow spheres. Adv Funct Mater, 2010, 20 (10): 1680—1686.

[7] Yang J, Takeda Y, Imanishi N, et al. Ultrafine Sn and $SnSb_{0.14}$ powders for lithium storage matrices in lithium-ion batteries. J Electrochem Soc, 1999, 146 (11): 4009—4013.

[8] Larcher D, Beattie S, Morcrette M, et al. Recent findings and prospects in the field of pure metals as negative electrodes for Li-ion batteries. J Mater Chem, 2007, 17: 3759—3772.

[9] Wang Y, Lee J Y, Zeng H C. Polycrystalline SnO_2 nanotubes prepared via infiltration casting of nanocrystallites and their electrochemical application. Chem Mater, 2005, 17 (15): 3899—3903.

[10] Guo Z P, Du G D, Nuli Y, et al. Ultra-fine porous SnO_2 nanopowder prepared via a molten salt process: a highly efficient anode material for lithium-ion batteries. J Mater Chem, 2009, 19: 3253—3257.

[11] Wang C, Zhou Y, Ge M Y, et al. Large-scale synthesis of SnO_2 nanosheets with high lithium storage capacity. J Am Chem Soc, 2010, 132 (1): 46—47.

[12] Park M S, Wang G X, Kang Y M, et al. Preparation and electrochemical properties of SnO_2 nanowires for application in lithium-ion batteries. Angew Chem Int Ed, 2007, 46 (5): 750—753.

[13] Guo Y G, Hu J S, Wan L J. Nanostructured materials for electrochemical energy conversion and storage devices. Adv Mater, 2008, 20 (15): 2878—2887.

[14] Lou X W, Li C M, Archer A L. Designed synthesis of coaxial SnO_2 carbon hollow nanospheres for highly reversible lithium storage. Adv Mater, 2009, 21 (24): 2536—2539.

[15] Wen Z H, Wang Q, Zhang Q, et al. In situ growth of mesoporous SnO_2 on multiwalled carbon nanotubes: a novel composite with porous-tube structure as anode for lithium batteries. Adv Funct Mater, 2007, 17 (15): 2772—2778.

[16] Wang Y, Zhang H J, Lu L, et al. Designed functional systems from peapod-like Co Carbon to Co_3O_4 carbon nanocomposites. ACS Nano, 2010, 4 (8): 4753—4761.

[17] Wang Z, Luan D, Madhavi S, et al. Assembling carbon-coated α-Fe_2O_3 hollow nanohorns on the CNT backbone for superior lithium storage capability. Energy Environ Sci, 2012, 5 (1): 5252—5256.

[18] Yang R, Zhao W, Zheng J, et al. One-step synthesis of carbon-coated tin dioxide nanoparticles for high lithium storage. J Phys Chem C, 2010, 114 (47): 20272—20276.

[19] Yuan L, Konstantinov K, Wang G X, et al. Nano-structured SnO_2-carbon composites obtained by in situ spray pyrolysis method as anodes in lithium batteries. J Power Sources, 2005, 146 (1—2): 180—184.

[20] Novoselov K S, Geim A K, Morozov S V, et al. Electric field effect in atomically thin carbon films. Science, 2004, 306 (5696): 666—669.

[21] Bolotin K I, Sikes K J, Jiang Z, et al. Ultrahigh electron mobility in suspended graphene. Solid State Commun, 2008, 146: 351—355.

[22] Novoselov K S, Geim A K, Morozov S V, et al. Two-dimensional gas of massless Dirac fermions in graphene. Nature, 2005, 438: 197—120.

[23] Zhang Y, Tan Y W, Stormer H L, et al. Experimental observation of the quantum Hall effect and Berry's phase in graphene. Nature, 2005, 438: 201—204.

[24] Lee C, Wei X, Kysar J W, et al. Measurement of the elastic properties and intrinsic strength of monolayer graphene. Science, 2008, 321 (5887): 385—388.

[25] Balandin A A, Ghosh S, Bao W, et al. Superior thermal conductivity of single-layer graphene. Nano Lett, 2008, 8 (3): 902—907.

[26] Gwon H, Kim H S, Lee K U, et al. Flexible energy storage devices based on graphene paper. Energy Environ Sci, 2011, 4 (4): 1277—1283.

[27] Courtney I A, Dahn J R. Key factors controlling the reversibility of the reaction of lithium with SnO_2 and Sn_2BPO_6 glass. J Electrochem Soc, 1997, 144 (9): 2943—2948.

[28] Park C M, Kim J H, Kim H, et al. Li-alloy based anode materials for Li secondary batteries. Chem Soc Rev, 2010, 39 (8): 3115—3141.

[29] Wu Z S, Zhou G, Yin L C, et al. Graphene/metal oxide composite electrode materials for energy storage. Nano Energy, 2012, 1 (1): 107—131.

[30] Liu J, Li W, Manthiram A. Dense core-shell structured SnO_2/C composites as high performance anodes for lithium ion batteries. Chem Commun, 2010, 46 (9): 1437—1439.

[31] Zhang H X, Feng C, Zhai Y C, et al. Cross-stacked carbon nanotube sheets uniformly loaded with SnO_2 nanoparticles: a novel binder-rree and high-capacity anode material for lithium-ion batteries. Adv Mater, 2009, 21 (22): 2299—2304.

[32] Shao Q G, Chen W M, Wang Z H, et al. SnO_2-based composite coaxial nanocables with multi-walled carbon nanotube and polypyrrole as anode materials for lithium-ion batteries. Electrochem Commun, 2011, 13 (12): 1431—1434.

[33] Idota Y, Kubota T, Matsufuji A, et al. Tin-based amorphous oxide: a high-capacity lithium-ion-storage material. Science, 1997, 276 (5317): 1395—1397.

[34] Paek S M, Yoo E, Honma I. Enhanced cyclic performance and lithium storage capacity of SnO_2/graphene nanoporous electrodes with three-dimensionally delaminated flexible structure. Nano Letters, 2009, 9 (1): 72—75.

[35] Yao J, Shen X P, Wang B, et al. In situ chemical synthesis of SnO_2-graphene nanocomposite as anode materials for lithium-ion batteries. Electrochem Commun, 2009, 11 (10): 1849—1852.

[36] Li Y M, Lv X J, Lu J, et al. Preparation of SnO_2-nanocrystal/graphene-nanosheets composites and their lithium storage ability. J Phys Chem C, 2010, 114 (49): 21770—21774.

[37] Zhang M, Lei D N, Du Z F, et al. Fast synthesis of SnO_2/graphene composites by reducing graphene oxide with stannous ions. J Mater Chem, 2011, 21: 1673—1676.

[38] Wang X Y, Zhou X F, Yao K, et al. A SnO_2/graphene compositeas a high stability electrode for lithium ion batteries. Carbon, 2011, 49 (1): 133—139.

[39] Liang J, Wei W, Zhong D, et al. One-step in situ synthesis of SnO_2/graphene nanocomposites and its application as an anode material for Li-ion batteries. ACS Appl Mater Interfaces, 2012, 4 (1): 454—459.

[40] Zhou X, Wan L J, Guo Y G. Binding SnO_2 nanocrystals in nitrogen-doped graphene sheets as anode materials for lithium-ion batteries. Adv Mater, 2013, 25 (15): 2152--2157.

[41] Prabakar S J R, Hwang Y H, Bae E G, et al. SnO_2/graphene composites with self-assembled alternating oxide and amine layers for high Li-storage and excellent stability. Adv Mater, 2013, 25 (24): 3307—3312.

[42] Wang L, Wang D, Dong Z, et al. Interface chemistry engineering for stable cycling of reduced GO/SnO_2 nanocomposites for lithium ion battery. Nano Lett, 2013, 13 (4): 1711—1716.

[43] Ding S J, Luan D Y, Boey F Y C, et al. SnO_2 nanosheets grown on graphene sheets with enhanced lithium storage properties. Chem Commun, 2011, 47 (25): 7155—7157.

[44] Kim H, Kim S W, Park Y U, et al. SnO_2/graphene composite with high lithium storage capability for lithium rechargeable batteries. Nano Res, 2010, 3 (11): 813—821.

[45] Xu C H, Sun J, Gao L. Direct growth of monodisperse SnO_2 nanorods on graphene as high capacity anode materials for lithium ion batteries. J Mater Chem, 2012, 22: 975—979.

[46] Zhou X S, Yin Y X, Wan L J, et al. A robust composite of SnO_2 hollow nanospheres enwrapped by graphene as a high-capacity anode material for lithium-ion batteries. J Mater Chem, 2012, 22: 17456—17459.

[47] Tarascon J M, Armand M. Issues and challenges facing rechargeable lithium batteries. Nature, 2001, 414: 359—367.

[48] Chan C K, Peng H L, Liu G, et al. High-performance lithium battery anodes using silicon nanowires. Nat Nanotechnol, 2008, 3: 31—35.

[49] Li N, Chen Z, Ren W, et al. Flexible graphene-based lithium ion batteries with ultrafast charge and discharge rates. Proc Natl Acad Sci U S A, 2012, 109 (43): 17360—17365.

[50] Liang J, Zhao Y, Guo L, et al. Flexible free-standing graphene/SnO_2 nanocomposites paper for Li-ion battery. ACS Appl Mater Interfaces, 2012, 4 (11), 5742—5748.

[51] Wang X, Cao X Q, Bourgeois L, et al. N-doped graphene-SnO_2 sandwich paper for high-performance lithium-ion batteries. Adv Funct Mater, 2012, 22 (13): 2682—2690.

[52] Chen W, Li S, Chen C, et al. Self-assembly and embedding of nanoparticles by in situ reduced graphene for preparation of a 3D graphene/nanoparticle aerogel. Adv Mater, 2011, 23 (47): 5679—5683.

[53] Liang J, Liu Y, Guo L, et al. Facile one-step synthesis of a 3D macroscopic SnO_2-graphene aerogel and its application as a superior anode material for Li-ion batteries. RSC Adv, 2013, 3 (29): 11489—11492.

[54] Huang Y, Wu D, Han S, et al. Assembly of tin oxide/graphene nanosheets into 3D hierarchical frameworks for high-performance lithium storage. ChemSusChem, 2013, 6 (8): 1510—1515.

[55] Larcher D, Bonnin D, Cortes R, et al. Combined XRD, EXAFS, and Mössbauer studies of the reduction by lithium of α-Fe_2O_3 with various particle sizes. J Electrochem Soc, 2003, 150 (12): A1643- A1650.

[56] Zhang M, Qu B, Lei D, et al. A green and fast strategy for the scalable synthesis of Fe_2O_3/graphene with significantly enhanced Li-ion storage properties. J Mater Chem, 2012, 22: 3868—3874.

[57] Zhu X, Zhu Y, Murali S, et al. Nanostructured reduced graphene oxide/Fe_2O_3 composite as a high-performance anode material for lithium ion batteries. ACS Nano, 2011, 5 (4): 3333—3338.

[58] Du M, Xu C, Sun J, et al. Synthesis of α-Fe_2O_3 nanoparticles from $Fe(OH)_3$ sol and their composite with reduced graphene oxide for lithium ion batteries. J Mater Chem A, 2013, 1 (24): 7154—7158.

[59] Chen D, Quan H, Liang J, et al. One-pot synthesis of hematite graphene core shell nanostructures for superior lithium storage. Nanoscale, 2013, in press, DOI: 10.1039/C3NR03484D.

[60] Yang S, Feng X, Ivanovici S, et al. Fabrication of graphene-encapsulated oxide nanoparticles: towards high-performance anode materials for lithium storage. Angew Chem Int Ed, 2010, 49 (45): 8408—8411.

[61] Wu Z S, Ren W, Wen L, et al. Graphene anchored with Co_3O_4 nanoparticles as anode of lithium ion batteries with enhanced reversible capacity and cyclic performance. ACS Nano, 2010, 4 (6): 3187—3194.

[62] Chen S Q, Wang Y. Microwave-assisted synthesis of a Co_3O_4-graphene sheet-on-sheet nanocomposite as a superior anode material for Li-ion batteries. J Mater Chem, 2010, 20: 9735—9739.

[63] Li B, Cao H, Shao J, et al. Co_3O_4 graphene composites as anode materials for high-performance lithium ion batteries. Inorg Chem, 2011, 50 (5): 1628—1632.

[64] Zou Y, Wang Y. NiO nanosheets grown on graphene nanosheets as superior anode materials for Li-ion batteries. Nanoscale, 2011, 3 (6): 2615—2620.

[65] Kottegoda I R M, Idris N H, Lu L, et al. Synthesis and characterization of graphene-nickel oxide nanostructures for fast charge-discharge application. Electrochim Acta, 2011, 56 (16): 5815—5822.

[66] Wang B, Wu X L, Shu C Y, et al. Synthesis of CuO/graphene nanocomposite as a high-performance anode material for lithium-ion batteries. J Mater Chem, 2010, 20: 10661—10664.

[67] Mai Y J, Wang X L, Xiang J Y, et al. CuO/graphene composite as anode materials for lithium-ion batteries. Electrochim Acta, 2011, 56 (5): 2306—2311.

[68] Lu L Q, Wang Y. Sheet-like and fusiform CuO nanostructures grown on graphene by rapid microwave heating for high Li-ion storage capacities. J Mater Chem, 2011, 21: 17916 17921.

[69] Wang H, Cui L F, Yang Y, et al. Mn_3O_4-graphene hybrid as a high-capacity anode material for lithium ion batteries. J Am Chem Soc, 2010, 132 (40): 13978—13980.

[70] Yu A, Park H W, Davies A, et al. Free-standing layer-by-layer hybrid thin film of graphene-MnO_2 nanotube as anode for lithium ion batteries. J Phys Chem Lett, 2011, 2 (15): 1855 1860.

[71] Guo C X, Wang M, Chen T, et al. A hierarchically nanostructured composite of MnO_2/conjugated polymer/graphene for high-performance lithium ion batteries. Adv Energy Mater, 2011, 1 (5): 736—741.

[72] Hsieh C T, Lin C Y, Lin J Y. High reversibility of Li intercalation and de-intercalation in MnO-attached graphene anodes for Li-ion batteries. Electrochim Acta, 2011, 56 (24): 8861 8867.

[73] Li L, Guo Z, Du A, et al. Rapid microwave-assisted synthesis of Mn_3O_4-graphene nanocomposite and its lithium storage properties. J Mater Chem, 2012, 22: 3600- 3605.

Guo Lin

Prof. Guo Lin graduated from the East North Normal University of China in 1985, received his Master's Degree in physics chemistry at Jilin University in 1992 and Ph. D. in materials science and engineering at Beijing Institute of Technology in 1997. He was a postdoctoral fellow at Institute of High Energy Physics, Chinese Academy of Sciences (CAS) from 1997 to 1998 for 20 months, and a visiting scholar in Hong Kong University of Science and Technology from 1999 to 2000. He is the Director of Center of Chemistry and Vice Dean of School of Chemistry and Environment, Beihang University. He has published more than 170 papers in peer-reviewed journals. He won the Humboldt Fellowship Award in 2001, Ministry of Education of the People's Republic of China Prize for Outstanding Young Teacher in 2001, the Program for New Century Excellent Talents in University in 2004. He was granted the National Science Fund for Distinguished Young Scholars in 2007, and Cheung Kong scholar Professor in 2011.